Journal of Biomedical Optics

BiomedicalOptics.SPIEDigitalLibrary.org

Optimization of sample cooling temperature for redox cryo-imaging

Anle Wang
Jing Yuan
Weihua Luo
Mengmeng Liu
Qingming Luo

SPIE.

Optimization of sample cooling temperature for redox cryo-imaging

Anle Wang,[a,b] Jing Yuan,[a,b] Weihua Luo,[a,b] Mengmeng Liu,[a,b] and Qingming Luo[a,b,*]
[a]Huazhong University of Science and Technology, Wuhan National Laboratory for Optoelectronics, Britton Chance Center for Biomedical Photonics, 1037 Luoyu Road, Wuhan 430074, China
[b]Huazhong University of Science and Technology, MoE Key Laboratory for Biomedical Photonics, School of Optical and Electronic Information HUST, 1037 Luoyu Road, Wuhan 430074, China

Abstract. Cryo-imaging techniques have been widely used to measure the metabolic state of tissues by capturing reduced nicotinamide adenine dinucleotide (NADH) and flavin adenine dinucleotide (FAD) autofluorescence. However, NADH and FAD fluorescence is sensitive to changes in temperature, which may result in unreliable redox ratio calculations. Here, the relationship between the measured redox ratio and sample surface temperature was analyzed using a standard phantom solution and biological tissues. The results indicated that a temperature < -100°C was a suitable cryo-imaging temperature window in which redox ratio measuring was immune to temperature fluctuations. These results may serve as a reference for designing and optimizing redox cryo-imaging experiments for quantitatively mapping the metabolic state of biological samples. [DOI: 10.1117/1.JBO.19.8.080502]

Keywords: metabolism; redox ratio; cryo-imaging; temperature window; reduced nicotinamide adenine dinucleotide; flavin adenine dinucleotide.

Paper 140334LR received May 30, 2014; revised manuscript received Jul. 15, 2014; accepted for publication Jul. 16, 2014; published online Aug. 22, 2014.

Cryo-imaging has been widely used for its high fluorescent quantum yield,[1] molecule stability, and three-dimensional (3-D) imaging capability.[2] It is an ideal technique with which to visualize metabolism, because low temperatures inactivate metabolic reactions[3] and allow one to obtain *in vivo* snapshots of the highly dynamic metabolic state. Reduced nicotinamide adenine dinucleotide (NADH) and flavin adenine dinucleotide (FAD) are two coenzymes of the mitochondrial respiratory chain that are highly autofluorescent. The redox ratio, calculated using the relative fluorescence intensities of the coenzymes, has been recognized as a useful indicator of the cellular or tissue metabolic state in cryo-imaging studies.[4,5]

Temperature control is a central problem in cryo-imaging techniques. There are two methods for creating the low-temperature environment for cryo-imaging: cooling either by liquid nitrogen[3] or an electrical freezer.[6] Maintaining the sample at a low temperature is necessary to stabilize chemical reactions; however, the current cooling systems have vast temperature differences (−195.8°C compared to −17°C). Very little is known regarding whether NADH and FAD are properly stabilized or if their measurements are comparable between the two temperature conditions.[1,7]

There are three primary sources of signal instability in redox cryo-imaging. First, since the NADH and FAD molecules are highly dynamic coenzymes, the precise temperature required to stop NADH and FAD reactions or movement within a tissue is unknown. Second, the NADH and FAD autofluorescence signals have been shown to increase with a temperature decrease because of molecular conformational changes, changes in solvent polarity, or other unknown reasons.[8] Finally, during measurement, the sample is often sequentially sectioned for 3-D imaging. Mechanical friction can generate heat on the sample surface and, thus, the local sample temperature may fluctuate. Hence, to confirm the effect of temperature on NADH and FAD emission intensities and their mitochondrial redox ratio, we used a standard phantom solution and biological tissues and investigated the signal stability of redox cryo-imaging during temperature change.

A homemade wide-field cryo-imaging testing system was employed to simultaneously measure the redox ratio and sample surface temperature, as shown in Fig. 1. An illumination unit combined light from 365- and 455-nm light-emitting diodes (Edmund Optics, Barrington) together to provide shadow-free, cool, uniform, and direct illumination of the sample surface. NADH and FAD fluorescence signals were collected with two emission filters (447/60 nm, 536/40 nm, Edmund Optics) and detected by a CCD camera (Retiga 4000DC, Surrey and Canada, Qimaging, mounted on an Olympus SZX10 microscope). The sample was mounted vertically in a customized sample box filled with liquid nitrogen. The block face of the sample was obtained by horizontal cutting and kept above the liquid nitrogen level to ensure image quality during the experiment. A temperature sensor (Pt100, Beijing and China, BJZYHS) directly contacted the sample surface to record the surface temperature in real time. As liquid nitrogen in the sample box vaporized, the sample temperature gradually increased. NADH and FAD images were captured alternately at different temperatures and the real-time temperature of the sample surface was simultaneously recorded.

Image data were analyzed by customized MATLAB® programs. Pixel values from a region of interest (ROI) of each image were averaged as the fluorescent intensity of the sample. As the metabolic state and intrinsic fluorophore concentrations varied between samples, all NADH and FAD fluorescence intensities were normalized to the maximum signal value of each channel. Alternate data acquisition modes and continuous temperature elevation resulted in NADH and FAD fluorescent images that may not have been captured at the same temperature points. Thus, spline interpolation[9] was used to obtain NADH (or FAD) image data at the same temperature points as an FAD (or NADH) image in order to calculate the redox ratio. The redox ratio, r, was calculated as follows:[10]

$$r = \frac{I_{\mathrm{FAD}}}{I_{\mathrm{FAD}} + I_{\mathrm{NADH}}}, \tag{1}$$

where I_{FAD} and I_{NADH} are the normalized fluorescence intensities of FAD and NADH, respectively. In order to compare the temperature-dependent behavior of different biological

*Address all correspondence to: Qingming Luo, E-mail: qluo@mail.hust.edu.cn

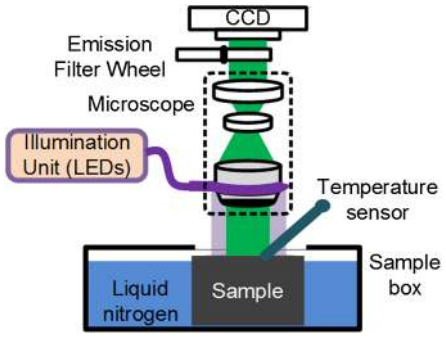

Fig. 1 Homemade redox cryo-imaging system.

tissues, the redox ratio measurements of all samples were normalized by

$$r_{\text{nor}} = \frac{r - r_{\text{min}}}{r_0 - r_{\text{min}}}, \tag{2}$$

where r_{nor} is the normalized redox ratio, r_0 represents the redox ratio at the initial temperature point, and r_{min} is the minimal redox ratio measured over the course of the experiment.

The rat experimental protocols were approved by the Internal Animal Care and Use Committee of the Huazhong University of Science and Technology. Cryo-fixation of rat brain tissue was performed by a funnel cryo-fixation protocol.[11] Temporal muscles were dissected from the organism and immediately immersed in liquid nitrogen.

We first used four mixtures of 0.5 mM NADH and FAD (powder from Sigma-Aldrich, St. Louis, in Tris-HCl buffer) as standard phantom solutions in 1-mm internal diameter glass tubes to test the redox measurement sensitivity. The initial temperature of the sample surface was −175°C. While both NADH and FAD signals decreased as the sample warmed, their profiles were significantly different [Figs. 2(a) and 2(b), respectively]. Both fluorescent intensities initially continuously decreased until the sample surface temperature reached −100°C. While the NADH curve plateaued between −100 and −50°C, the FAD intensity continued to decrease linearly. The decline in intensity of both fluorescent signals continued until −15°C. The calculated redox ratio was also sensitive to temperature change [Fig. 2(c)]. This experiment demonstrates that there are two stages of sample surface temperature effects on redox ratio measurement. In the first stage, at ultralow temperatures, the redox ratio fell slowly with increased temperature, while in the second stage, at low temperatures, the redox ratio declined quickly. To describe this trend more clearly, the critical temperature point between the first and second stages was defined as the temperature point at which the decline in the amplitude of the redox ratio was 10% of the whole decrease in redox ratio amplitude over the experimental temperature range. The critical temperature was −100°C for the standard phantom solution. The redox ratio continued to decrease by 76%, until −25°C, at a rate of 1% decrease in redox ratio per 1°C increase.

To test the effect of temperature on redox ratios calculated from biological samples, we performed redox cryo-imaging experiments in rat brain and temporal muscle. Their redox ratios were calculated using Eq. (1) and normalized by Eq. (2), and are shown in Fig. 3. The trend of the normalized redox ratio decreased as the sample surface temperature increased and was similar for all samples tested. The critical temperature points for rat brain and muscle curves were −90°C and −88°C, respectively. The nonlinear curves of best fit for the brain and muscle

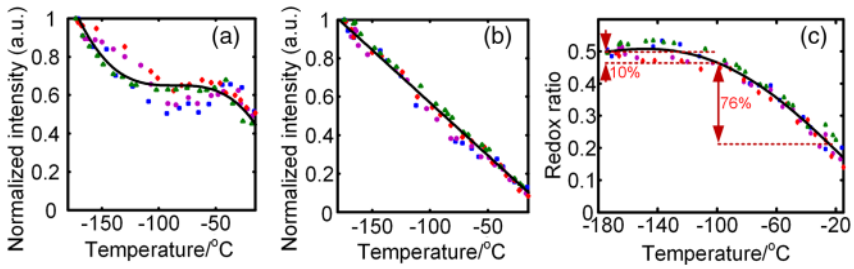

Fig. 2 Effects of sample surface temperature on fluorescent intensities of (a) reduced nicotinamide adenine dinucleotide and (b) flavin adenine dinucleotide, as well as (c) the calculated redox ratio of the standard phantom solution. Four signs and black lines represent measurements of the four samples and the corresponding curves of best fit.

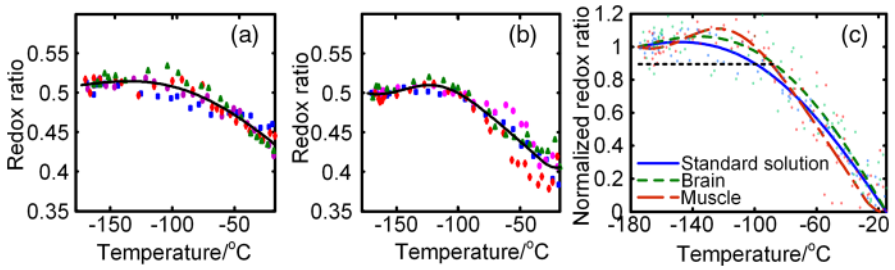

Fig. 3 Effect of sample surface temperature on redox ratios of (a) brain ($N = 4$) and (b) muscle ($N = 4$), as well as (c) the normalized redox ratios calculated from the standard phantom solution (blue symbols and solid line), rat brain (green symbols and dot line), and muscle (red symbols and dot dash line). Different colorful symbols represent different specimens in (a) and (b).

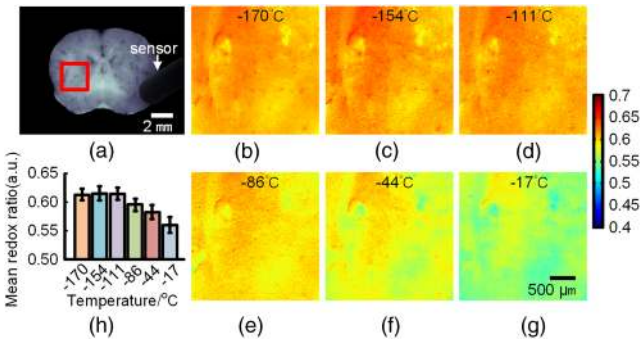

Fig. 4 Temperature influence on the redox ratio in the rat brain. (a) The region of interest (ROI) selected from the whole coronal section. (b) to (g) Redox ratio measurements of the ROI at different temperatures. (h) Bar graph plot comparing the mean values from (b) to (g).

were different from that of the standard phantom solution. This may have been caused by complex autofluorescent components in biological tissue with different fluorescence-temperature sensitivity profiles.[12]

To further test the sensitivity of redox cryo-imaging to sample temperature, we compared the redox ratio from a group of coronal images from rat brains at different low temperature points (Fig. 4). Redox ratio images of an ROI in Fig. 4(a) at six different temperature points are presented in Figs. 4(b)–4(g). The mean redox ratio of each image is illustrated in Fig. 4(h). The average redox ratios of the former three images were 0.6121, 0.6152, and 0.6133, respectively, with a range of 0.0031. In comparison, the average redox ratios of the latter three images declined by 0.0363 from 0.5963 to 0.5600. This decrease in redox ratio as sample temperature increased is consistent with the results from Figs. 2 and 3.

In summary, we employed a standard phantom solution and biological tissues to study the effects of sample temperature on redox ratio measurement by cryo-imaging. The results revealed that at ultralow temperatures < -100°C, redox ratio measurements are immune to temperature fluctuation, while cryo-imaging experiments performed at higher temperatures require more stable and precise cooling equipment to quantitatively acquire and compare the metabolic states between different samples. In addition, the robustness of the redox rate calculation to temperature fluctuations in the ultralow temperature range increases the system tolerance for temperature instability in different experiments. Our results will be helpful for designing new cryo-imaging systems and improving the quantitative power of current cryo-imaging systems.

Acknowledgments

This work was supported by PhD Programs Foundation of Ministry of Education of China (Grant No. 20110142130006), National Natural Science Foundation of China (Grant Nos. 81171067, 91232000 and 61205197) and National Key Technology R&D Program (Grant No. 2012BAI08B04). The authors thank Drs. Lin Li and Shoko Nioka for critical reviews. We also appreciate the Optical Bioimaging Core Facility of WNLO-HUST and the Analytical and Testing Center of HUST.

References

1. B. Chance et al., "Oxidation-reduction ratio studies of mitochondria in freeze-trapped samples. NADH and flavoprotein fluorescence signals," *J. Biol. Chem.* **254**(11), 4764–4771 (1979).
2. D. Roy et al., "3D cryo-imaging: a very high-resolution view of the whole mouse," *Anat. Rec.* **292**(3), 342–351 (2009).
3. B. Quistorff, J. C. Haselgrove, and B. Chance, "High spatial resolution readout of 3-D metabolic organ structure: an automated, low-temperature redox ratio-scanning instrument," *Anal. Biochem.* **148**(2), 389–400 (1985).
4. A. Shiino et al., "Poor recovery of mitochondrial redox state in CA1 after transient forebrain ischemia in gerbils," *Stroke* **29**(11), 2421–2424, discussion 2425 (1998).
5. M. Ranji et al., "Quantifying acute myocardial injury using ratiometric fluorometry," *IEEE Trans. Biomed. Eng.* **56**(5), 1556–1563 (2009).
6. R. Sepehr et al., "Optical imaging of tissue mitochondrial redox state in intact rat lungs in two models of pulmonary oxidative stress," *J. Biomed. Opt.* **17**(4), 046010 (2012).
7. F. A. Welsh and W. Rieder, "Evaluation of in situ freezing of cat brain by NADH fluorescence," *J. Neurochem.* **31**(1), 299–309 (1978).
8. J. R. Lakowicz, *Principles of Fluorescence Spectroscopy*, Springer, New York, NY (2007).
9. C. De Boor, *A Practical Guide to Splines*, Springer-Verlag, New York (1978).
10. L. Z. Li et al., "Mitochondrial redox imaging for cancer diagnostic and therapeutic studies," *J. Innov. Opt. Health Sci.* **2**(04), 325–341 (2009).
11. N. Sun et al., "Quality evaluation method for rat brain cryofixation on the basis of NADH fluorescence," in *Oxygen Transport to Tissue XXXV*, S. Van Huffel et al., Eds., pp. 435–440, Springer, New York (2013).
12. I. E. Hassinen, "From identification of fluorescent flavoproteins to mitochondrial redox indicators in intact tissues," *J. Innov. Opt. Health Sci.* **7**(2), 1350058 (2013).